Journal of Sound and Vibration (1999) **228**(3), 569–588
Article No. jsvi.1999.2425, available online at http://www.idealibrary.com on IDEAL®

FULLY COUPLED BUFFETING ANALYSIS OF LONG-SPAN CABLE-SUPPORTED BRIDGES: FORMULATION

D. K. Sun, Y. L. Xu and J. M. Ko

Department of Civil and Structural Engineering, The Hong Kong Polytechnic University, Hung Hom, Kowloon, Hong Kong

AND

J. H. Lin

Research Institute of Engineering Mechanics, Dalian University of Technology, Dalian, People's Republic of China

(*Received* 17 *March* 1999, *and in final form* 1 *June* 1999)

A formulation for fully coupled buffeting analysis of long-span cable-supported bridges is presented, in which dynamic coupling between modes of vibration, dynamic forces on bridge deck and towers and cables, and varying wind speed and structural properties along the bridge deck and towers and cables can be taken into consideration. This formulation adopts a finite element approach and a pseudo-excitation method. Aeroelastic forces on the bridge deck are changed into nodal forces to form aeroelastic damping and stiffness matrices while aerodynamic forces on the bridge deck, towers and cables are converted into nodal forces to obtain a loading vector. After the system equation of motion is assembled, the pseudo-excitation method is applied and the formulation is programmed so that a personal computer can be used to execute the buffeting analysis of the system of hundreds of degrees of freedom in 1 or 2 h. The results from the case study of a long suspension bridge using the proposed formulation and program are also selectively presented in this paper.

1. INTRODUCTION

Wind-induced vibrations of the bridge deck of a long-span cable-supported bridge are classified mainly as buffeting, vortex shedding, flutter and galloping. Many efforts have been made in last two decades to successfully prevent bridge deck from flutter instability through the optimization of deck cross-section and/or the installation of aeroelastic devices. The optimization of deck cross-section has also significantly reduced vortex-shedding response. Relatively less attention has been given to the buffeting response of bridge decks, probably because the buffeting response does not generally lead to catastrophic failure. However, with the record-breaking span lengths of modern long-span cable-supported bridges, the

0022-460X/99/480569 + 20 $30.00/0

buffeting response is significantly increased, which may lead to serious fatigue damage to structural components and connections, instability of vehicles travelling on the deck, and discomfort to pedestrian.

In the early 1960s, Davenport [1] applied statistical concepts of the stationary time series and random vibration theory to the buffeting analysis of long-span bridges. He introduced aerodynamic admittance functions and joint acceptances to consider the temporal and spatial distributions of aerodynamic forces along the bridge deck. He also partly took account of motion effects of bridge deck on buffeting response using aerodynamic damping. In the 1970s, Scanlan and Gade [2] extended their research results from flutter instability to buffeting response. They believed that aeroelastic forces in flutter instability would affect the buffeting response of the bridge deck, and hence they suggested that the aerodynamic forces due to wind turbulence be considered together with the aeroelastic forces due to the motion of the deck in the buffeting analysis of the bridge. In the aeroelastic forces they suggested, both aeroelastic stiffness and damping effects and aeroelastic coupling between flexural and torsional vibrations were included in terms of a set of flutter derivatives. In the aerodynamic forces, however, they did not consider the aerodynamic admittance functions.

The buffeting analysis of modern long-span bridges using either Davenport's theory or Scanlan's theory is actually a combination of numerical, experimental, and analytical approaches. The finite element technique is usually adopted to determine the natural frequencies and mode shapes of a modern long-span bridge. The wind tunnel tests of bridge section models provide flutter derivatives and aerodynamic coefficients. The buffeting response of the bridge deck is then determined using the SRSS method (the square root of the sum of squares of modal responses).

Modern long-span cable-supported bridges tend to have closely spaced natural frequencies. The contributions from multi-modes of vibration and inter-modes of vibration to the buffeting response, therefore, may have to be included. To consider the multi-mode buffeting response of a bridge deck, Lin and Yang [3] proposed a general linear theory for the computation of cross-spectra of the deck response to turbulent wind. Jain *et al.* [4] considered both multi-mode and inter-mode buffeting responses using a random vibration-based mode superposition approach. Katsuchi *et al.* [5] analyzed the Akashi–Kaikyo bridge, the longest suspension bridge in the world, using the multi-mode approach in reference [4] and demonstrated the significance of multi-mode responses of the bridge.

The wind-induced dynamic responses of bridge deck, towers and cables are traditionally determined separately to simplify the problem. Thus, wind-induced dynamic forces on the towers and cables are not considered in the aforementioned work. Recently, with respect to flutter instability of cable-stayed bridges, Ogawa *et al.* [6] pointed out that the ignorance of interaction between bridge deck, towers and cables may positively or negatively affect the prediction of flutter instability of a bridge. Davenport [7] also mentioned several possible mechanisms of interaction between the bridge deck and the cables.

In terms of modern computer technology, a fully coupled three-dimensional buffeting analysis of a long-span bridge is presented in this paper. The advantages

of the suggested approach, comprising a three-dimensional finite element approach and a pseudo-excitation method, are: (1) to readily handle the bridge deck with significantly varying structural properties and mean wind speed along the deck; (2) to make good use of the ready-made finite element models of the bridge for both static and eigenvalue analyses as well as the relevant results; (3) to naturally include inter-mode and multi-mode responses; (4) to determine wind-induced responses of the bridge deck, towers, and cables simultaneously; and (5) to lay down a foundation for investigation of vibration mitigation or control of cable-supported bridges.

2. AEROELASTIC STIFFNESS AND DAMPING MATRICES

Aeroelastic forces on a bridge deck come from the interaction between the wind flow and the motion of the deck. Scanlan and his co-workers [4, 8, 9] mathematically described the aeroelastic forces per unit length on a bridge deck in terms of the so-called flutter derivatives as follows:

$$D^{ae} = \frac{1}{2}\rho U^2 B_d \left[KP_1^* \frac{\dot{p}}{U} + KP_2^* \frac{B_d \dot{\alpha}}{U} + K^2 P_3^* \alpha + K^2 P_4^* \frac{p}{B_d} + KP_5^* \frac{\dot{h}}{U} + K^2 P_6^* \frac{h}{B_d} \right], \tag{1}$$

$$L^{ae} = \frac{1}{2}\rho U^2 B_d \left[KH_1^* \frac{\dot{h}}{U} + KH_2^* \frac{B_d \dot{\alpha}}{U} + K^2 H_3^* \alpha + K^2 H_4^* \frac{h}{B_d} + KH_5^* \frac{\dot{p}}{U} + K^2 H_6^* \frac{p}{B_d} \right], \tag{2}$$

$$M^{ae} = \frac{1}{2}\rho U^2 B_d^2 \left[KA_1^* \frac{\dot{h}}{U} + KA_2^* \frac{B_d \dot{\alpha}}{U} + K^2 A_3^* \alpha + K^2 A_4^* \frac{h}{B_d} + KA_5^* \frac{\dot{p}}{U} + K^2 A_6^* \frac{p}{B_d} \right], \tag{3}$$

where D^{ae}, L^{ae}, and M^{ae} are the aeroelastic drag, lift, and torsional moment, respectively, on the deck segment of unit length, ρ is the air density, U is the mean velocity of the incident wind at the deck segment, B_d is the width of the bridge deck segment, K is equal to $B_d\omega/U$ (called the reduced frequency), P_i^*, H_i^*, and A_i^* ($i = 1$–6) are the functions of $2\pi/K$ (called the flutter derivatives), $p(t)$, $h(t)$, and $\alpha(t)$ are the lateral, vertical, and angular dynamic displacements of the deck segment, respectively, and each over-dot denotes one partial differentiation with respect to time. There are some discussions on the application of equations (1)–(3) to the bridge deck, such as turbulent effects on flutter derivatives [10] and the spanwise diminution of coherence in the associated flutter derivatives [11]. These discussions are, however, not addressed in this study.

In a matrix notation, equations (1)–(3) can be expressed as

$$\mathbf{F}^{ae} = \mathbf{S}^{ae}\mathbf{d} + \mathbf{D}^{ae}\dot{\mathbf{d}}, \tag{4}$$

where

$$\mathbf{F}^{ae} = \begin{Bmatrix} D^{ae} \\ L^{ae} \\ M^{ae} \end{Bmatrix}, \qquad \mathbf{d} = \begin{Bmatrix} p \\ h \\ \alpha \end{Bmatrix}, \qquad \dot{\mathbf{d}} = \begin{Bmatrix} \dot{p} \\ \dot{h} \\ \dot{\alpha} \end{Bmatrix}, \tag{5}$$

$$\mathbf{S}^{ae} = \begin{bmatrix} C_{1,d}K^2P_4^* \dfrac{1}{B_d} & C_{1,d}K^2P_6^* \dfrac{1}{B_d} & C_{1,d}K^2P_3^* \\ C_{1,d}K^2H_6^* \dfrac{1}{B_d} & C_{1,d}K^2H_4^* \dfrac{1}{B_d} & C_{1,d}K^2H_3^* \\ C_{2,d}K^2A_6^* \dfrac{1}{B_d} & C_{2,d}K^2A_4^* \dfrac{1}{B_d} & C_{2,d}K^2A_3^* \end{bmatrix}, \tag{6}$$

$$\mathbf{D}^{ae} = \begin{bmatrix} C_{1,d}KP_1^* \dfrac{1}{U} & C_{1,d}KP_5^* \dfrac{1}{U} & C_{1,d}KP_2^* \dfrac{B_d}{U} \\ C_{1,d}KH_5^* \dfrac{1}{U} & C_{1,d}KH_1^* \dfrac{1}{U} & C_{1,d}KH_2^* \dfrac{B_d}{U} \\ C_{2,d}KA_5^* \dfrac{1}{U} & C_{2,d}KA_1^* \dfrac{1}{U} & C_{2,d}KA_2^* \dfrac{B_d}{U} \end{bmatrix}, \tag{7}$$

in which $C_{1,d} = \frac{1}{2}\rho U^2 B_d$, and $C_{2,d} = \frac{1}{2}\rho U^2 B_d^2$.

Assume that the bridge deck is modelled by three-dimensional beam elements, and the relation between the internal displacements of the ith element and its nodal displacements can be expressed as

$$\mathbf{d}_i = \mathbf{B}_i \mathbf{d}_i^e, \tag{8}$$

where the vector $\mathbf{d}_i$ is the 3×1 internal displacement vector of the ith deck element, corresponding to the vector $\mathbf{d}$, in the local co-ordinate system denoted by $\bar{x}$, $\bar{y}$, $\bar{z}$; the vector $\mathbf{d}_i^e$ is the 12×1 local nodal displacement vector of the ith deck element, and the matrix $\mathbf{B}_i$ is the 3×12 interpolation function matrix of the beam element. By using the principle of virtual work the aeroelastic stiffness and damping matrices of the ith element can then be, respectively, expressed as

$$\mathbf{K}_i^{ae} = \int_{L_i} \mathbf{B}_i^T \mathbf{S}_i^{ae} \mathbf{B}_i \, \mathrm{d}\bar{x}, \tag{9}$$

$$\mathbf{C}_i^{ae} = \int_{L_i} \mathbf{B}_i^T \mathbf{D}_i^{ae} \mathbf{B}_i \, \mathrm{d}\bar{x}, \tag{10}$$

where the integrals are definite integrals over the element length. If the length of the element is sufficiently small, the width of the element, the flutter derivatives, and the

mean wind speed for the element can be regarded as constant with respect to the local co-ordinate $\bar{x}$. Thus, after the integration of equations (9) and (10), either the aeroelastic element stiffness or the aeroelastic damping matrices can be expressed as a 12×12 matrix, as listed in Appendix A.

The system aeroelastic stiffness matrix $\mathbf{K}_s^{ae}$ and aeroelastic damping matrix $\mathbf{C}_s^{ae}$ can be assembled from the element aeroelastic stiffness and damping matrices in the same way as the system structural stiffness matrix $\mathbf{K}_s^s$ and structural damping matrix $\mathbf{C}_s^s$ are assembled from the element structural stiffness and damping matrices. The aeroelastic stiffness and damping matrices are different from the structural stiffness and damping matrices in which the former are the functions of both the frequency and the mean wind speed.

It may be worthwhile to point out that the aeroelastic stiffness and damping matrices described above have been used by some researchers to carry out finite element-based flutter analysis of cable-supported bridges [12–14]. However, to the best of writers' knowledge, they are not aware that anyone has used the combination of the finite element approach and pseudo-excitation method for the buffeting analysis of long-span cable-supported bridges.

3. AERODYNAMIC FORCES DUE TO TURBULENCE

3.1. AERODYNAMIC FORCES ON DECK

By assuming no interaction between aeroelastic and aerodynamic forces and by using quasi-steady aerodynamic force coefficients, the aerodynamic forces (buffeting forces) on the deck segment of unit length are expressed as [4, 9]

$$D_d^b = \frac{1}{2}\rho U^2 B_d \left[C_{D,d}\left(2\frac{u}{U}\right) + C'_{D,d}\frac{w}{U}\right], \tag{11}$$

$$L_d^b = \frac{1}{2}\rho U^2 B_d \left[C_{L,d}\left(2\frac{u}{U}\right) + (C'_{L,d} + C_{D,d})\frac{w}{U}\right], \tag{12}$$

$$M_d^b = \frac{1}{2}\rho U^2 B_d^2 \left[C_{M,d}\left(2\frac{u}{U}\right) + C'_{M,d}\frac{w}{U}\right], \tag{13}$$

where D_d^b, L_d^b, and M_d^b are the buffeting drag, lift, and moments respectively, on the deck segment of unit length, $C_{D,d}$, $C_{L,d}$, and $C_{M,d}$ are the drag, lift, and moment coefficients, respectively, $C'_{D,d} = dC_{D,d}/d\alpha$, $C'_{L,d} = dC_{L,d}/d\alpha$, $C'_{M,d} = dC_{M,d}/d\alpha$, α is the angle of attack of normal incident wind referring to the horizontal plane of the deck segment, and $u(t)$ and $w(t)$ are the horizontal and vertical components of fluctuating wind respectively.

The aerodynamic forces on the deck segment can also be expressed in matrix notation:

$$\mathbf{F}_d^b = \mathbf{A}_d^b \mathbf{q} \tag{14}$$

in which

$$\mathbf{F}_d^b = \begin{Bmatrix} \mathbf{D}_d^b \\ \mathbf{L}_d^b \\ \mathbf{M}_d^b \end{Bmatrix}, \qquad \mathbf{q} = \begin{Bmatrix} u \\ w \end{Bmatrix}, \qquad \mathbf{A}_d^b = \begin{bmatrix} C_{1,d}\left(\dfrac{2C_{D,d}}{U}\right) & C_{1,d}\left(\dfrac{C'_{D,d}}{U}\right) \\ C_{1,d}\left(\dfrac{2C_{L,d}}{U}\right) & C_{1,d}\left(\dfrac{C'_{L,d}+C_{D,d}}{U}\right) \\ C_{2,d}\left(\dfrac{2C_{M,d}}{U}\right) & C_{2,d}\left(\dfrac{C'_{M,d}}{U}\right) \end{bmatrix}. \tag{15}$$

The consistent buffeting forces at the nodal points of the ith deck element in the local coordinate system can be obtained by the following definite integral:

$$\mathbf{P}_{i,d}^b = \int_{L_i} \mathbf{B}_i^T \mathbf{A}_{i,d}^b \mathbf{q}_i \, \mathrm{d}\bar{x}. \tag{16}$$

If the length of the element is sufficiently small, the aerodynamic coefficients and their derivatives, the wind velocities for the element, and the width of the element can be regarded as constant along the element. Consequently, the buffeting forces at the nodal points of the ith deck element can be expressed as

$$\mathbf{P}_{i,d}^b = \mathbf{E}_{i,d}^b \mathbf{q}_i. \tag{17}$$

The expression of the matrix $\mathbf{E}_{i,d}^b$ is listed in Appendix B.

3.2. AERODYNAMIC FORCES ON TOWERS

The aerodynamic forces on a bridge tower caused by along-wind and cross-wind turbulence can be derived based on the quasi-steady assumption in a similar way to the aerodynamic forces on the bridge deck. Following the work of Davenport [15] and Solari [16], the aerodynamic forces on the bridge tower can be expressed in a general form as

$$\mathbf{F}_t^b = \mathbf{A}_t^b \mathbf{r} \tag{18}$$

in which

$$\mathbf{F}_t^b = \begin{Bmatrix} \mathbf{D}_t^b \\ \mathbf{L}_t^b \\ \mathbf{M}_t^b \end{Bmatrix}, \qquad \mathbf{r} = \begin{Bmatrix} u \\ v \end{Bmatrix}, \qquad \mathbf{A}_t^b = \begin{bmatrix} C_{1,t}\left(\dfrac{2C_{D,t}}{U}\right) & C_{1,t}\left(\dfrac{C'_{D,t}}{U}\right) \\ C_{1,t}\left(\dfrac{2C_{L,t}}{U}\right) & C_{1,t}\left(\dfrac{C'_{L,t}}{U}\right) \\ C_{2,t}\left(\dfrac{2C_{M,t}}{U}\right) & C_{2,t}\left(\dfrac{C'_{M,t}}{U}\right) \end{bmatrix}, \tag{19}$$

where D_t^b, L_t^b, and M_t^b are the buffeting drag, lift, and moment, respectively, on the tower segment of unit height, $C_{D,t}$, $C_{L,t}$, and $C_{M,t}$ are the buffeting drag, lift, and moment coefficients referring to the width B_t of the tower segment, $C'_{D,t} = \mathrm{d}C_{D,t}/\mathrm{d}\varphi$, $C'_{L,t} = \mathrm{d}C_{L,t}/\mathrm{d}\phi$, $C'_{M,t} = \mathrm{d}C_{M,t}/\mathrm{d}\phi$, ϕ is the angle of attack of normal

incident wind referring to the vertical plane of the tower segment, $u(t)$ and $v(t)$ are the horizontal and lateral components of fluctuating wind, respectively, and $C_{1,t} = \frac{1}{2}\rho U^2 B_t$, and $C_{2,t} = \frac{1}{2}\rho U^2 B_t^2$. Obviously, equation (19) is similar to equation (15) but for the tower, the aerodynamic coupling between lift and drag is ignored. The further hypothesis that $u(t)$ and $v(t)$ are statistically independent random processes was suggested by Solari [16] while Davenport [15] set $C'_{D,t}$ to zero.

The bridge tower is usually modelled as a series of three-dimensional beam elements. The consistent buffeting forces at the nodal points of the ith element in the local co-ordinate system for the bridge tower can be obtained by the following definite integral.

$$\mathbf{P}_{i,t}^b = \int_{L_i} \mathbf{B}_i^T \mathbf{A}_{i,t}^b \mathbf{r}_i \, \mathrm{d}\bar{x}. \tag{20}$$

Again, if the length of the tower element is sufficiently small, the aerodynamic coefficients and their derivatives, the wind velocities for the element, and the width of the element can be regarded as constant along the element. Consequently, the buffeting forces at the nodal points of the ith tower element can be expressed as

$$\mathbf{P}_{i,t}^b = \mathbf{E}_{i,t}^b \mathbf{r}_i. \tag{21}$$

The expression of the matrix $\mathbf{E}_{i,t}^b$ is listed in Appendix B.

3.3. AERODYNAMIC FORCES ON CABLES

In the eigenvalue analysis of the bridge, the cable is usually modelled as a series of two-node cable elements. In accordance with this arrangement and the quasi-steady assumption, the aerodynamic forces on the cable segment of unit length due to turbulence can be written as

$$\mathbf{F}_c^b = \mathbf{A}_c^b \mathbf{u} \tag{22}$$

in which

$$\mathbf{F}_c^b = \begin{Bmatrix} D_c^b \\ L_c^b \end{Bmatrix}, \qquad \mathbf{A}_c^b = \begin{Bmatrix} C_{1,c}\left(\dfrac{2C_{D,c}}{U}\right) \\ C_{1,c}\left(\dfrac{2C_{L,c}}{U}\right) \end{Bmatrix}, \tag{23}$$

where D_c^b and L_c^b are the buffeting drag and lift, respectively, on the bridge cable segment of unit height, $C_{D,c}$ and $C_{L,c}$ are the drag and lift coefficients referring to the dominant dimension B_c of the cable segment, and if the cable has a circular section, the lift coefficient is regarded as zero, and $C_{1,c} = \frac{1}{2}\rho U^2 B_c$.

The consistent buffeting forces at the nodal points of the ith cable element in the local co-ordinate system for the bridge cable can be obtained by the following definite integral:

$$\mathbf{P}_{i,c}^b = \int_{L_i} \mathbf{B}_{i,c}^T \mathbf{A}_{i,c}^b u_i \, \mathrm{d}\bar{x}, \tag{24}$$

in which $\mathbf{B}_{i,c}$ is the 2×6 interpolation function matrix for the cable element. Assuming that the structural properties and wind properties are constant with respect to the element, the buffeting forces at the nodal points of the ith cable element can be expressed as

$$\mathbf{P}_{i,c}^{b} = \mathbf{E}_{i,c}^{b} u_i. \tag{25}$$

The expression of the matrix $\mathbf{E}_{i,c}^{b}$ is listed in Appendix B.

4. LOADING SPECTRAL DENSITY FUNCTION MATRIX

The nodal forces obtained by equations (17), (21) and (25) are in the local co-ordinate systems. They should be converted to those in the global co-ordinate system through the co-ordinate transformation matrix $\mathbf{T}_i$ used in the eigenvalue analysis of the bridge:

$$\mathbf{P}_{i,s}^{b} = \mathbf{T}_i \mathbf{P}_{i,e}^{b}, \tag{26}$$

where $\mathbf{P}_{i,e}^{b}$ can be either the aerodynamic forces on the deck element $\mathbf{P}_{i,d}^{b}$ or the aerodynamic forces on the tower element $\mathbf{P}_{i,t}^{b}$ or on the cable element $\mathbf{P}_{i,c}^{b}$; $\mathbf{P}_{i,s}^{b}$ is the nodal force vector of the ith element in the global co-ordinate system with the same dimension as the system nodal force vector, and $\mathbf{T}_i$ is the co-ordinate transformation matrix with the dimensions equal to the dimension of the system nodal force vector times, 12 for a beam element or 6 for a cable element. As a result, the global (system) aerodynamic force vector, including the bridge deck and towers and cables, can be obtained by

$$\mathbf{P}_{s}^{b} = \sum_{i}^{n} \mathbf{P}_{i,s}^{b} = \sum_{i}^{n} \mathbf{T}_i \mathbf{P}_{i,e}^{b} = \mathbf{T}\mathbf{P}^{g}, \tag{27}$$

where

$$\mathbf{T} = [\mathbf{T}_1, \mathbf{T}_2, \ldots, \mathbf{T}_i, \ldots, \mathbf{T}_n], \tag{28}$$

$$\mathbf{P}^{g^{\mathrm{T}}} = \{\mathbf{P}_{1,e}^{b^{\mathrm{T}}}, \mathbf{P}_{2,e}^{b^{\mathrm{T}}}, \ldots, \mathbf{P}_{i,e}^{b^{\mathrm{T}}}, \ldots, \mathbf{P}_{n,e}^{b^{\mathrm{T}}}\}^{T}, \tag{29}$$

where the superscript T means the transposition of a matrix and n is the total number of the elements subject to wind loading. Notice that the co-ordinate transformation matrix $\mathbf{T}$ is not a function of t. Therefore, if assuming that the fluctuating wind components $u(t)$, $v(t)$, and $w(t)$ acting on the elements can be represented by a stationary random process, the correlation function matrix for the buffeting forces on the whole bridge can be obtained by

$$E[\mathbf{P}_{s}^{b}(t_1)\mathbf{P}_{s}^{b^{\mathrm{T}}}(t_2)] = \mathbf{T}E[\mathbf{P}^{g}(t_1)\mathbf{P}^{g^{\mathrm{T}}}(t_2)]\mathbf{T}^{\mathrm{T}}$$

$$= \mathbf{T}\begin{bmatrix} E[\mathbf{P}_{1,e}^{b}(t_1)\mathbf{P}_{1,e}^{b^{\mathrm{T}}}(t_2)] & E[\mathbf{P}_{1,e}^{b}(t_1)\mathbf{P}_{2,e}^{b^{\mathrm{T}}}(t_2)] & \cdots & E[\mathbf{P}_{1,e}^{b}(t_1)\mathbf{P}_{n,e}^{b^{\mathrm{T}}}(t_2)] \\ E[\mathbf{P}_{2,e}^{b}(t_1)\mathbf{P}_{1,e}^{b^{\mathrm{T}}}(t_2)] & E[\mathbf{P}_{2,e}^{b}(t_1)\mathbf{P}_{2,e}^{b^{\mathrm{T}}}(t_2)] & \cdots & E[\mathbf{P}_{2,e}^{b}(t_1)\mathbf{P}_{n,e}^{b^{\mathrm{T}}}(t_2)] \\ \vdots & \vdots & \ddots & \vdots \\ E[\mathbf{P}_{n,e}^{b}(t_1)\mathbf{P}_{1,e}^{b^{\mathrm{T}}}(t_2)] & E[\mathbf{P}_{n,e}^{b}(t_1)\mathbf{P}_{2,e}^{b^{\mathrm{T}}}(t_2)] & & E[\mathbf{P}_{n,e}^{b}(t_1)\mathbf{P}_{n,e}^{b^{\mathrm{T}}}(t_2)] \end{bmatrix}\mathbf{T}^{\mathrm{T}}, \tag{30}$$

where E is the expected value operator. The spectral density function matrix of the nodal buffeting forces acting on the whole bridge in the global co-ordinate system is thus

$$\mathbf{S}^b_{pp}(\omega) = \mathbf{T}\begin{bmatrix} \mathbf{S}^e_{p_1p_1}(\omega) & \mathbf{S}^e_{p_1p_2}(\omega) & \cdots & \mathbf{S}^e_{p_1p_n}(\omega) \\ \mathbf{S}^e_{p_2p_1}(\omega) & \mathbf{S}^e_{p_2p_2}(\omega) & \cdots & \mathbf{S}^e_{p_2p_n}(\omega) \\ \vdots & \vdots & \ddots & \cdots \\ \mathbf{S}^e_{p_np_1}(\omega) & \mathbf{S}^e_{p_np_2}(\omega) & & \mathbf{S}^e_{p_np_n}(\omega) \end{bmatrix}\mathbf{T}^{\mathrm{T}}. \tag{31}$$

The cross-spectral density function matrix of the nodal buffeting forces acting on the ith and jth elements can be expressed in a general form as

$$\mathbf{S}^e_{P_iP_j}(x_i, x_j, z_i, z_j, \omega) = \mathbf{E}_i(z_i)\mathbf{S}_{ij}(x_i, x_j, z_i, z_j, \omega)\ [\mathbf{E}_j(z_j)]^{\mathrm{T}}. \tag{32}$$

If both the ith and jth elements are deck elements, $\mathbf{S}^e_{p_ip_j}(x_i, x_j, z_i, z_j, \omega)$ is the 12×12 cross-spectral density function matrix, $\mathbf{E}_k(z_k) = \mathbf{E}^b_{k,d}(z_k)$, $k = i, j$, and

$$\mathbf{S}_{ij}(x_i, x_j, z_i, z_j, \omega) = \begin{bmatrix} S_{uu}(x_i, x_j, z_i, z_j, \omega) & S_{uw}(x_i, x_j, z_i, z_j, \omega) \\ S_{wu}(x_i, x_j, z_i, z_j, \omega) & S_{ww}(x_i, x_j, z_i, z_j, \omega) \end{bmatrix}. \tag{33}$$

in which x_i and z_i, and x_j and z_j can be selected as the global co-ordinates of the midpoint of the ith and the jth bridge deck element, respectively.

If both the ith and jth elements are tower elements, $\mathbf{S}^e_{p_ip_j}(x_i, x_j, z_i, z_j, \omega)$ is also the 12×12 cross-spectral density function matrix, $\mathbf{E}_k(z_k) = \mathbf{E}^b_{k,t}(z_k)$, $k = i, j$, and

$$\mathbf{S}_{ij}(x_i, x_j, z_i, z_j, \omega) = \begin{bmatrix} S_{uu}(x_i, x_j, z_i, z_j, \omega) & S_{uv}(x_i, x_j, z_i, z_j, \omega) \\ S_{vu}(x_i, x_j, z_i, z_j, \omega) & S_{vv}(x_i, x_j, z_i, z_j, \omega) \end{bmatrix}. \tag{34}$$

If both the ith and jth elements are cable elements, $\mathbf{S}^e_{p_ip_j}(x_i, x_j, z_i, z_j, \omega)$ is the 6×6 cross-spectral density function matrix; $\mathbf{E}_k(z_k) = \mathbf{E}^b_{k,c}(z_k)$, $k = i, j$, and

$$S_{ij}(x_i, x_j, z_i, z_j, \omega) = S_{uu}(x_i, x_j, z_i, z_j, \omega). \tag{35}$$

If the ith element is a deck element and the jth element is a cable element, $\mathbf{S}^e_{p_ip_j}(x_i, x_j, z_i, z_j, \omega)$ is the 12×6 cross-spectral density function matrix, $\mathbf{E}_i(z_i) = \mathbf{E}^b_{i,d}(z_i)$, $\mathbf{E}_j(z_j) = \mathbf{E}^b_{j,c}(z_j)$, and

$$\mathbf{S}_{ij}(x_i, x_j, z_i, z_j, \omega) = \begin{Bmatrix} S_{uu}(x_i, x_j, z_i, z_j, \omega) \\ S_{wu}(x_i, x_j, z_i, z_j, \omega) \end{Bmatrix}. \tag{36}$$

Similar explanation can be given to the two elements of which one is a tower element and the other is a cable element or to the two elements of which one is a tower element and the other is a deck element.

The cross-spectral density functions of the wind components on the elements in reference [9] are adopted:

$$S_{uu}(x_i, x_j, z_i, z_j, \omega) = \sqrt{\frac{200u^2_* f(z_i)}{\omega/2\pi(1 + 50f(z_i))^{5/3}}}\sqrt{\frac{200u^2_* f(z_j)}{\omega/2\pi(1 + 50f(z_j))^{5/3}}}\,\mathrm{e}^{-\gamma(p_i,\ p_j)}, \tag{37}$$

$$S_{vv}(x_i, x_j, z_i, z_j, \omega) = \sqrt{\frac{15u_*^2\ f(z_i)}{\omega/2\pi(1 + 9{\cdot}5f(z_i))^{5/3}}}\ \sqrt{\frac{15u_*^2\ f(z_j)}{\omega/2\pi(1 + 9{\cdot}5f(z_j))^{5/3}}}\ \mathrm{e}^{-\gamma(p_i,\ p_j)}, \tag{38}$$

$$S_{ww}(x_i, x_j, z_i, z_j, \omega) = \sqrt{\frac{3{\cdot}36u_*^2\ f(z_i)}{\omega/2\pi(1 + 10f(z_i)^{5/3})}}\ \sqrt{\frac{3{\cdot}36u_*^2\ f(z_j)}{\omega/2\pi(1 + 10f(z_j)^{5/3})}}\ \mathrm{e}^{-\gamma(p_i,\ p_j)}, \tag{39}$$

$$S_{k,l}(x_i, x_j, z_i, z_j, \omega) = C_{k,l}(x_i, x_j, z_i, z_j, \omega) + \mathrm{i}Q_{k,l}(x_i, x_j, z_i, z_j, \omega), \tag{40}$$

$$S_{k,l}(x_i, x_j, z_i, z_j, \omega) = S_{l,k}^*(x_i, x_j, z_i, z_j, \omega), \quad k \neq l \text{ and } k, l = u, v, w \tag{41}$$

in which,

$$f(z_k) = \frac{\omega z_k}{2\pi U(z_k)}, \tag{42}$$

$$\gamma(p_i, p_j) = \frac{\omega[C_x^2(x_i - x_j)^2 + C_y^2(y_i - y_j)^2 + C_z^2(z_i - z_j)^2]^{1/2}}{\pi[U(z_i) + U(z_j)]}, \tag{43}$$

where C_x, C_y, and C_z are the constants determined experimentally. For the deck elements, it is suggested that $5KL_d/2\pi B_d \leqslant C_x \leqslant 20KL_d/2\pi B_d$ be satisfied. L_d is the total length of the bridge deck, u_* is the friction velocity of the wind, i is the imaginary unit, $C_{k,l}$ and $Q_{k,l}$ are the co-spectra and quadrature spectra, respectively, and $S_{k,l}^*$ is the conjugation of $S_{k,l}$. No quantitative assessment for the quadrature spectrum $Q_{k,l}$ has yet been made, but for the deck C_{uw} can be chosen as [4]

$$C_{uw}(x_i, x_j, z_i, z_j, \omega) = -\sqrt{\frac{14u_*^2 f(z_i)}{\omega/2\pi(1 + 9{\cdot}6f(z_i))^{2{\cdot}4}}}\ \sqrt{\frac{14u_*^2 f(z_j)}{\omega/2\pi(1 + 9{\cdot}6f(z_j))^{2{\cdot}4}}}\ \mathrm{e}^{-C_x|x_i - x_j|/L_d}. \tag{44}$$

5. PSEUDO-EXCITATION METHOD

The equation of motion of the whole bridge for the buffeting analysis can be expressed as

$$\mathbf{M}\ddot{\mathbf{Y}}(t) + \mathbf{C}\dot{\mathbf{Y}}(t) + \mathbf{K}\mathbf{Y}(t) = \mathbf{R}\mathbf{P}(t), \tag{45}$$

in which $\mathbf{Y}(t)$ is the total nodal displacement vector of N dimensions including the bridge deck, towers, cables, and other components, $\mathbf{M}$ is the $N \times N$ total mass matrix, $\mathbf{C}$ is the $N \times N$ total damping matrix which consists of both aeroelastic damping matrix $\mathbf{C}_s^{ae}$ and structural damping matrix $\mathbf{C}_s^s$, $\mathbf{K}$ is the $N \times N$ total stiffness matrix containing the aeroelastic stiffness matrix $\mathbf{K}_s^{ae}$ and the structural stiffness matrix $\mathbf{K}_s^s$, $\mathbf{P}$ is the total loading vector of m dimensions (in general, $m \ll N$), and it is equal to $\mathbf{P}_s^b$, $\mathbf{R}$ is the $N \times m$ matrix consisting of 0 and 1, which expands the m-dimensional loading vector into the N-dimensional loading vector.

The Fourier transformation of equation (45) gives the frequency-domain transfer function between loading and displacement response as

$$\mathbf{H}(\mathrm{i}\omega) = [-\omega^2\mathbf{M} + \mathrm{i}\omega\mathbf{C} + \mathbf{K}]^{-1}, \tag{46}$$

in which the superscript -1 means the matrix inversion. The spectral density function matrix for the displacement response can be then calculated from the spectral density function matrix of the buffeting force:

$$\mathbf{S}_{YY}(\omega) = \mathbf{H}^{*}\mathbf{R}\mathbf{S}_{PP}(\omega)\mathbf{R}^{\mathrm{T}}\mathbf{H}^{\mathrm{T}}. \tag{47}$$

The computation effort required for the determination of the response spectral density function matrix is tremendous for a long-span bridge if equation (47) is applied. Traditionally, the random-vibration-based mode superposition approach (the SRSS method) is used to overcome this problem if the natural frequencies of the bridge are well separated and the structural damping is small. For a long-span bridge of closely spaced natural frequencies, inter-mode and multi-mode responses may be important. A pseudo-excitation algorithm is thus suggested here to determine the spectral density function matrix for the buffeting response. This algorithm actually converts the random response calculation to the deterministic response calculation. The principle of the algorithm [17] and its application to wind-excited structures are introduced as follows:

Note that the spectral density function matrix $\mathbf{S}_{PP}(\omega)$ or $\mathbf{S}^{b}_{PP}(\omega)$ is a symmetric matrix. Therefore, this excitation spectral matrix can be decomposed as

$$\mathbf{S}_{PP}(\omega) = \mathbf{L}^{*}\mathbf{D}\mathbf{L}^{\mathrm{T}} \tag{48}$$

in which $\mathbf{L}$ is the lower triangular matrix and $\mathbf{D}$ the diagonal matrix. With the kth column of $\mathbf{L}$ denoted as $\mathbf{L}_k$ and the kth diagonal element of $\mathbf{D}$ denoted as d_{kk}, $\mathbf{S}_{PP}(\omega)$ can be further expressed as

$$\mathbf{S}_{PP}(\omega) = \sum_{k=1}^{m} d_{kk}\mathbf{L}_k^{*}\mathbf{L}_k^{\mathrm{T}}. \tag{49}$$

Let $S_{P_iP_i}(\omega)$ and L_{ik} denote the element in $\mathbf{S}_{PP}(\omega)$ at the ith row and ith column, and the ith element in the kth column $\mathbf{L}_k$ respectively. These elements can be then determined using the following procedure:

$$\mathrm{d}_{11} = \mathrm{S}_{p_1p_1}, \tag{50}$$

$$d_{ii} = S_{P_iP_i} - \sum_{r=1}^{i-1} \mathrm{L}_{ir}^{*}\mathrm{L}_{ir}\mathrm{d}_{rr}, \tag{51}$$

$$L_{ij} = \frac{1}{d_{jj}}\left(d_{ii} - \sum_{r=1}^{i-1} L_{ir}^{*}L_{jr}d_{rr}\right), \quad j < i, \tag{52}$$

$$L_{ij} = 0, \quad i < j. \tag{53}$$

Then, the pseudo-excitations are constituted as follows:

$$\mathbf{f}_k = \mathbf{L}_k \exp(\mathrm{i}\omega t) \quad (k = 1, 2, \ldots, m). \tag{54}$$

For each pseudo-excitation vector, a pseudo-displacement response vector, $\mathbf{Y}_k(\omega)$, can be determined by

$$\mathbf{Y}_k = \mathbf{H}(\omega)\mathbf{R}\mathbf{f}_k. \tag{55}$$

It can be readily proved that the spectral density function matrix of the displacement response of the bridge can be obtained by

$$\mathbf{S}_{YY}(\omega) = \sum_{k=1}^{m} d_{kk}\, \mathbf{Y}_k^* \mathbf{Y}_k^{\mathrm{T}}. \tag{56}$$

Much less computation effort is needed to calculate the response spectral density matrix by the pseudo-excitation method, equation (56), than by equation (47), in particular if the internal force response spectral density matrix is required. Further reduction of computation time can also be achieved if the buffeting response of a long-span bridge is dominated by the first few modes of vibration. In this case, the equation of motion, equation (45), can be first reduced from N dimensions to r dimensions in terms of the mode shapes found in the eigenvalue analysis, where r is the number of modes of vibration interested.

Let $\mathbf{Q}_{N\times r}$ be the modal matrix containing the first r mode shapes, and introduce a linear transformation.

$$\mathbf{Y}_{N\times 1} = \mathbf{Q}_{N\times r}\mathbf{z}_{r\times 1} \tag{57}$$

in which $\mathbf{z}$ is the $r\times 1$ generalised displacement response vector. Equation (45) of N dimensions can be reduced to the equation of r dimensions:

$$\mathbf{M}_r\ddot{\mathbf{z}}(t) + \mathbf{C}_r\dot{\mathbf{z}}(t) + \mathbf{K}_r\mathbf{z}(t) = \mathbf{P}_r(t), \tag{58}$$

where

$$\mathbf{M}_r = \mathbf{Q}^{\mathrm{T}}\mathbf{M}\mathbf{Q}, \qquad \mathbf{C}_r = \mathbf{Q}^{\mathrm{T}}\mathbf{C}\mathbf{Q}, \qquad \mathbf{K}_r = \mathbf{Q}^{\mathrm{T}}\mathbf{K}\mathbf{Q}, \qquad \mathbf{P}_r = \mathbf{Q}^{\mathrm{T}}\mathbf{R}\mathbf{P}. \tag{59}$$

The pseudo-excitations are computed according to

$$\mathbf{f}_{rk} = \mathbf{Q}^{\mathrm{T}}\mathbf{R}\mathbf{L}_k \exp(\mathrm{i}\omega t) \quad (k = 1, 2, \ldots, m). \tag{60}$$

For each pseudo-excitation vector, the pseudo-displacement response vector, $\mathbf{Y}_k(\omega)$, is now determined by

$$\mathbf{Y}_k = \mathbf{Q}\mathbf{H}_r(\omega)\mathbf{R}\mathbf{f}_{rk} \quad (k = 1, 2, \ldots, m), \tag{61}$$

where the transfer function is

$$\mathbf{H}_r(\mathrm{i}\omega) = [-\omega^2\mathbf{M}_r + \mathrm{i}\omega\mathbf{C}_r + \mathbf{K}_r]^{-1}. \tag{62}$$

The spectral density function matrix for the displacement response attributed to the first r modes of vibration is computed according to equations (56) and (61).

It is seen that different from the SRSS method, the pseudo-excitation method retains the cross-correlation terms between the first r normal modes. The modal coupling effects can thus be included. The standard deviations of the displacement, velocity, and acceleration of the node can be readily computed according to the random vibration theory, after the auto spectral density functions for each node are determined.

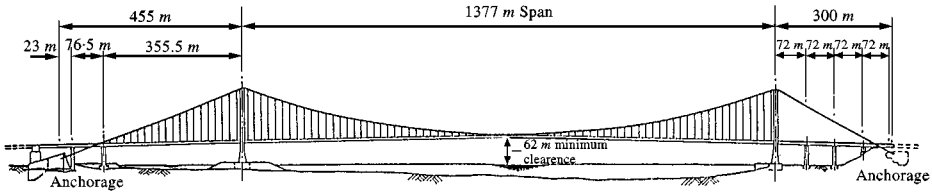

Figure 1. Configuration of long suspension bridge used in case study.

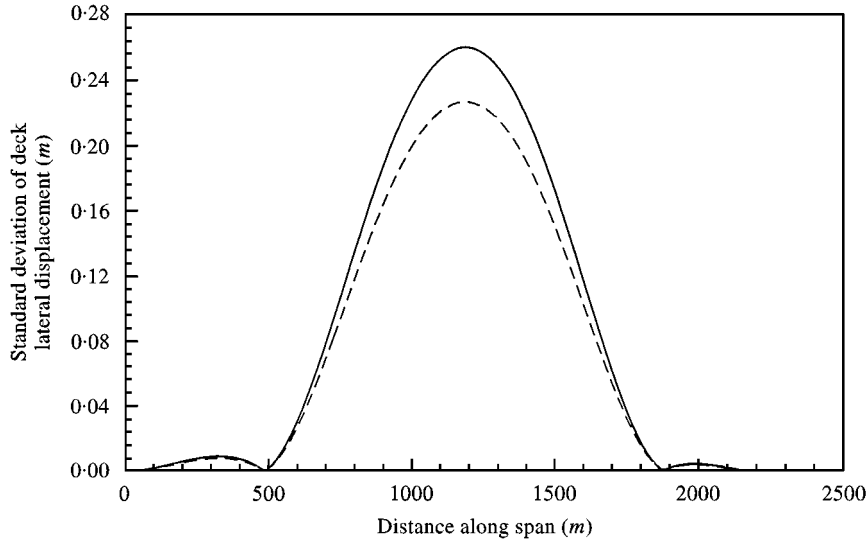

Figure 2. Lateral displacement response of bridge deck. (—) Full bridge; (– – –) deck only.

6. APPLICATION

The formulation described above was programmed and applied to a real long suspension bridge having a main span of 1377 m and two side spans of 300 and 350 m respectively (see Figure 1). The height of the tower is 206 m while the diameter of the main cable is 1·1 m. The bridge deck is a hybrid steel structure carrying both the highway and the railway. The modal analysis of the bridge showed that the natural frequencies of the bridge were spaced very closely; the first 20 natural frequencies ranged from 0·068 to 0·380 Hz only. The flutter derivatives H_i^* and $A_i^*(i = 1, 2, 3, 4)$ and the aerodynamic force coefficients of the bridge deck were measured from wind tunnel tests. The variation of mean wind speed with height was assumed to follow a power law with an exponent of 0·19 for an open terrain. The reference mean wind speed was taken as 25 m/s at the bridge deck level near the tower and the wind was assumed to be normal to the bridge deck.

Due to space limitation, most of the results from the case study will be presented later, together with the detailed information on the bridge structural system, bridge modal properties, flutter derivatives and aerodynamic parameters. Figure 2 shows the variations of standard deviation of deck lateral displacement response along the span for the full bridge and for the deck only. The term "full bridge" means that the

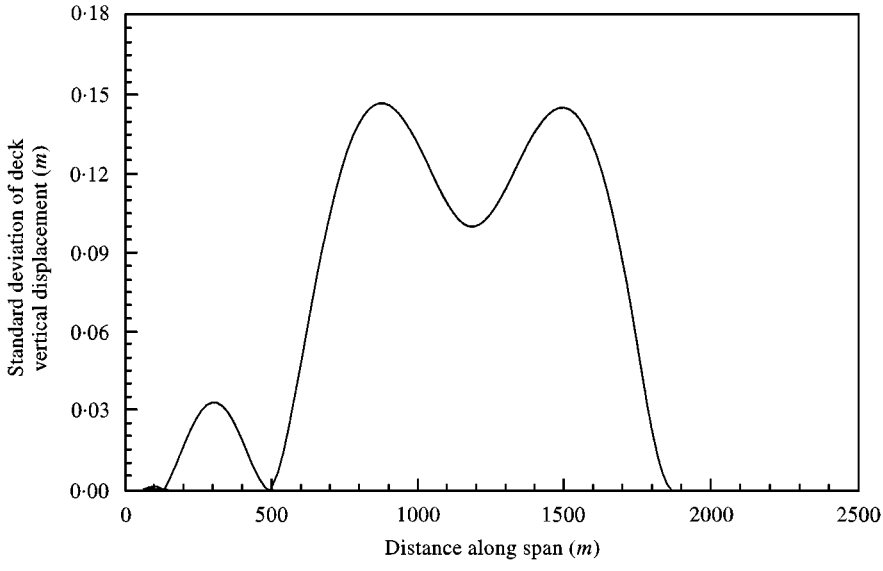

Figure 3. Vertical displacement response of bridge deck. (—) Full bridge; (– – –) deck only.

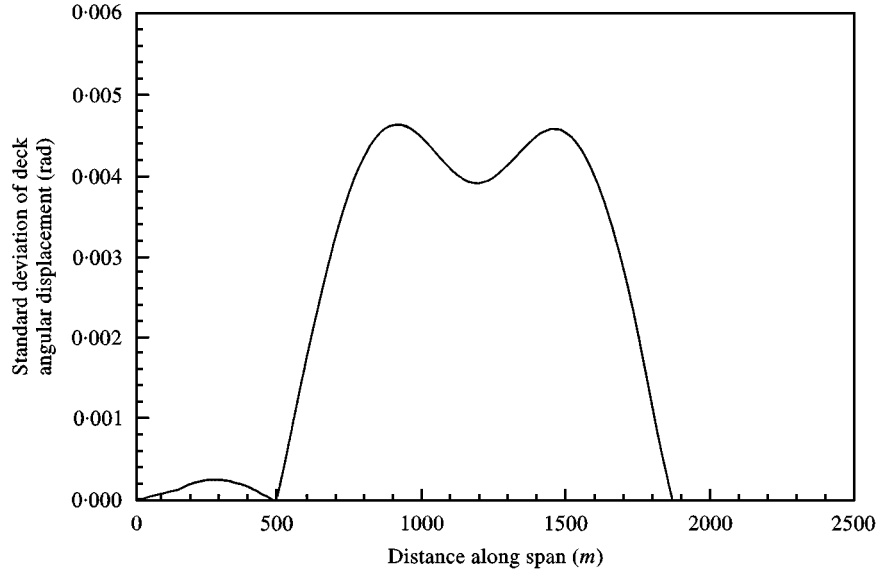

Figure 4. Angular displacement response of bridge deck. (—) Full bridge; (– – –) deck only.

buffeting forces not only on the bridge deck but also on the bridge towers and cables are included in the analysis. The term "deck only" implies buffeting forces only on the bridge deck and no buffeting forces on the bridge towers and cables in the analysis. It is seen from Figure 2 that due to the consideration of buffeting forces on the main cables and towers, the lateral displacement response of the bridge deck increases by about 15% at the midspan. The variations of standard deviation of deck vertical and angular displacement responses along the span for the full bridge, however, are almost the same as those for the deck only, as shown in Figures 3 and 4 respectively.

7. CONCLUSIONS

A new formulation has been presented in this paper for fully coupled three-dimensional buffeting analysis of long-span cable-supported bridges. The formulation is featured by a combination of the finite element approach and pseudo-excitation method. The advantages of the suggested formulation are: (1) to readily handle the bridge deck of significantly varying structural properties and mean wind speed along the deck; (2) to make good use of the ready-made finite element models of the bridge for both static and eigenvalue analyses; (3) to naturally include inter-mode and multi-mode responses; (4) to determine wind-induced responses of the bridge deck, towers, and cables simultaneously; and (5) to lay down a foundation for the investigation of vibration mitigation or control of cable-supported bridges.

The suggested formulation has been intentionally programmed so that a personal computer could be used to execute the buffeting analysis of the system of hundreds of degrees of freedom in 1 or 2 h. A case study of a real long suspension bridge has been carried out using the developed program and the results have been selectively presented. The case study, however, does not include effects of aerodynamic admittance, spatial correlation of flutter derivatives, lateral flutter derivatives, and others which need further investigation.

ACKNOWLEDGMENT

The writers are grateful for the financial supports from the Hong Kong Research Grant Council through a UGC grant.

REFERENCES

1. A. G. Davenport 1962 *Journal of Structural Division ASCE* **88**, 233–268. Buffeting of a suspension bridge by storm winds.
2. R. H. Scanlan and R. H. Gade 1977 *Journal of Structural Division ASCE* **103**, 1867–1883. Motion of suspended bridge spans under gusty wind.
3. Y. K. Lin and J. N. Yang 1983 *Journal of Engineering Mechanics ASCE* **109**, 586–603. Multimode bridge response to wind excitations.
4. A. Jain, N. P. Jones and R. H. Scanlan 1996 *Journal of Structural Engineering ASCE* **122**, 716–725. Coupled flutter and buffeting analysis of long-span bridges.
5. H. Katsuchi, N. P. Jones and R. H. Scanlan 1999 *Journal of Structural Engineering* **125**, 60–70. Multimode coupled flutter and buffeting analysis of the Akashi–Kaikyo bridge.
6. K. Ogawa, H. Shimodoi and H. Ishizaki 1992 *Journal of Wind Engineering and Industrial Aerodynamics* 41–44, 1227–1238. Aeroelastic stability of a cable-stayed bridge with girder, tower and cables.
7. A. G. Davenport 1994 *AFPC Conference, Deauville, France*, 427–437. A simple representation of the dynamics of a massive stay cable in wind.
8. R. H. Scanlan and N. P. Jones 1990 *Journal of Structural Engineering ASCE* **116**, 279–297. Aeroelastic analysis of cable-stayed bridges.
9. E. Simiu and R. H. Scanlan 1996 *Wind Effects on Structures*. New York: Wiley.
10. Y. K. Lin and Q. C. Li 1992 *Journal of Engineering Mechanics ASCE* **119**, 113–127. New stochastic theory for bridge stability in turbulent flow.

11. R. H. Scanlan 1997 *Journal of Structural Engineering ASCE* **123**, 232–236. Amplitude and turbulence effects on bridge flutter derivatives.
12. T. J. A. Agar 1991 *Computers and Structures* **41**, 1321–1328. Dynamic instability of suspension bridges.
13. A. Namini, P. Albrecht and H. Bosch 1992 *Journal of Structural Engineering* **118**, 1509–1526. Finite element-based flutter analysis of cable-suspension bridges.
14. M. S. Pfeil and R. C. Batista 1995 *Journal of Structural Engineering ASCE* **121**, 1784–1794. Aeroelastic stability analysis of cable-stayed bridges.
15. A. G. Davenport 1962 *Proceedings of Institution of Civil Engineers* **23**, 389–408. The response of slender line like structures to a gusty wind.
16. G. Solari 1985 *Journal of Engineering Mechanics ASCE* **111**, 254–276. Mathematical model to predict 3-D wind loading on buildings.
17. J. H. Lin 1992 *Computers and Structures* **4**, 683–687. A fast CQC algorithm of PSD matrices for random seismic responses.

APPENDIX A. AEROELASTIC ELEMENT STIFFNESS AND DAMPING MATRICES

The interpolation function matrix **B** used for a beam element is as follows:

$$\mathbf{B}=\begin{bmatrix} 0 & \psi_1 & 0 & 0 & 0 & \psi_3 & 0 & \psi_2 & 0 & 0 & 0 & \psi_4 \\ 0 & 0 & \psi_1 & 0 & -\psi_3 & 0 & 0 & 0 & \psi_2 & 0 & -\psi_4 & 0 \\ 0 & 0 & 0 & 1-x/L & 0 & 0 & 0 & 0 & 0 & x/L & 0 & 0 \end{bmatrix} \tag{A1}$$

in which

$$\psi_1(x)=1-3\left(\frac{x}{L}\right)^2+2\left(\frac{x}{L}\right)^3, \qquad \psi_2(x)=3\left(\frac{x}{L}\right)^2-2\left(\frac{x}{L}\right)^3,$$

$$\psi_3(x)=x\left(1-\frac{x}{L}\right)^2, \qquad \psi_4(x)=\frac{x^2}{L}\left(\frac{x}{L}-1\right). \tag{A2}$$

The aeroelastic stiffness coefficients in the 12×12 aeroelastic stiffness matrix, $\mathbf{K}^{ae}$, for the deck element can thus be obtained according to equation (9):

$$K^{ae}_{1,j}=0, \quad (j=1,2,\ldots,12), \qquad K^{ae}_{7,j}=0, \quad (j=1,2,\ldots,12),$$

$$K^{ae}_{j,1}=0, \quad (j=1,2,\ldots,12), \qquad K^{ae}_{j,7}=0, \quad (j=1,2,\ldots,12),$$

$$K^{ae}_{2,2}=\tfrac{13}{35}LS^{ae}_{1,1}, \quad K^{ae}_{2,3}=\tfrac{13}{35}LS^{ae}_{1,2}, \quad K^{ae}_{2,4}=\tfrac{7}{20}LS^{ae}_{1,3}, \quad K^{ae}_{2,5}=\tfrac{13}{210}L^2S^{ae}_{1,2},$$

$$K^{ae}_{2,6}=-\tfrac{13}{210}L^2S^{ae}_{1,1},$$

$$K^{ae}_{2,8}=\tfrac{19}{70}LS^{ae}_{1,1}, \quad K^{ae}_{2,9}=\tfrac{19}{70}LS^{ae}_{1,2}, \quad K^{ae}_{2,10}=\tfrac{3}{20}LS^{ae}_{1,3}, \quad K^{ae}_{2,11}=\tfrac{13}{210}L^2S^{ae}_{1,2},$$

$$K^{ae}_{2,12}=-\tfrac{13}{210}L^2S^{ae}_{1,1},$$

$$K^{ae}_{3,2}=\tfrac{13}{35}LS^{ae}_{2,1}, \quad K^{ae}_{3,3}=\tfrac{13}{35}LS^{ae}_{2,2}, \quad K^{ae}_{3,4}=\tfrac{7}{20}LS^{ae}_{2,3}, \quad K^{ae}_{3,5}=\tfrac{13}{210}L^2S^{ae}_{2,2},$$

$$K^{ae}_{3,6} = -\tfrac{13}{210} L^2 S^{ae}_{2,1},$$

$$K^{ae}_{3,8} = \tfrac{19}{70} L S^{ae}_{2,1}, \quad K^{ae}_{3,9} = \tfrac{19}{70} L S^{ae}_{2,2}, \quad K^{ae}_{3,10} = \tfrac{3}{20} L S^{ae}_{2,3}, \quad K^{ae}_{3,11} = \tfrac{13}{210} L^2 S^{ae}_{2,2},$$

$$K^{ae}_{3,12} = -\tfrac{13}{210} L^2 S^{ae}_{2,1},$$

$$K^{ae}_{4,2} = \tfrac{7}{20} L S^{ae}_{3,1}, \quad K^{ae}_{4,3} = \tfrac{7}{20} L S^{ae}_{3,2}, \quad K^{ae}_{4,4} = \tfrac{1}{3} L S^{ae}_{3,3}, \quad K^{ae}_{4,5} = -\tfrac{21}{20} L^2 S^{ae}_{3,2},$$

$$K^{ae}_{4,6} = \tfrac{21}{20} L^2 S^{ae}_{3,1},$$

$$K^{ae}_{4,8} = \tfrac{3}{20} L S^{ae}_{3,1}, \quad K^{ae}_{4,9} = \tfrac{3}{20} L S^{ae}_{3,2}, \quad K^{ae}_{4,10} = \tfrac{1}{6} L S^{ae}_{3,3}, \quad K^{ae}_{4,11} = \tfrac{1}{30} L^2 S^{ae}_{3,2},$$

$$K^{ae}_{4,12} = -\tfrac{1}{30} L^2 S^{ae}_{3,1},$$

$$K^{ae}_{5,2} = \tfrac{13}{210} L^2 S^{ae}_{2,1}, \quad K^{ae}_{5,3} = \tfrac{13}{210} L^2 S^{ae}_{2,2}, \quad K^{ae}_{5,4} = -\tfrac{21}{20} L^2 S^{ae}_{2,3},$$

$$K^{ae}_{5,5} = \tfrac{1}{105} L^3 S^{ae}_{2,2}, \quad K^{ae}_{5,6} = \tfrac{1}{105} L^3 S^{ae}_{2,1},$$

$$K^{ae}_{5,8} = -\tfrac{3}{70} L^2 S^{ae}_{2,1}, \quad K^{ae}_{5,9} = -\tfrac{3}{70} L^2 S^{ae}_{2,2}, \quad K^{ae}_{5,10} = -\tfrac{1}{30} L^2 S^{ae}_{2,3},$$

$$K^{ae}_{5,11} = -\tfrac{1}{140} L^2 S^{ae}_{2,2}, \quad K^{ae}_{5,12} = \tfrac{1}{140} L^2 S^{ae}_{2,1},$$

$$K^{ae}_{6,2} = -\tfrac{13}{210} L^2 S^{ae}_{1,1}, \quad K^{ae}_{6,3} = -\tfrac{13}{210} L^2 S^{ae}_{1,2}, \quad K^{ae}_{6,4} = \tfrac{21}{20} L^2 S^{ae}_{1,3},$$

$$K^{ae}_{6,5} = -\tfrac{1}{105} L^3 S^{ae}_{1,2}, \quad K^{ae}_{6,6} = \tfrac{1}{105} L^3 S^{ae}_{1,1},$$

$$K^{ae}_{6,8} = \tfrac{3}{70} L^2 S^{ae}_{1,1}, \quad K^{ae}_{6,9} = \tfrac{3}{70} L^2 S^{ae}_{1,2}, \quad K^{ae}_{6,10} = \tfrac{1}{30} L^2 S^{ae}_{1,3}, \quad K^{ae}_{6,11} = \tfrac{1}{140} L^2 S^{ae}_{1,2},$$

$$K^{ae}_{6,12} = -\tfrac{1}{140} L^2 S^{ae}_{1,1},$$

$$K^{ae}_{8,2} = \tfrac{19}{70} L S^{ae}_{1,1}, \quad K^{ae}_{8,3} = \tfrac{19}{70} L S^{ae}_{1,2}, \quad K^{ae}_{8,4} = \tfrac{3}{20} L S^{ae}_{1,3}, \quad K^{ae}_{8,5} = -\tfrac{3}{70} L^2 S^{ae}_{1,2},$$

$$K^{ae}_{8,6} = \tfrac{3}{70} L^2 S^{ae}_{1,1},$$

$$K^{ae}_{8,8} = \tfrac{13}{35} L S^{ae}_{1,1}, \quad K^{ae}_{8,9} = \tfrac{13}{35} L S^{ae}_{1,2}, \quad K^{ae}_{8,10} = \tfrac{7}{20} L S^{ae}_{1,3}, \quad K^{ae}_{8,11} = \tfrac{19}{140} L^2 S^{ae}_{1,2},$$

$$K^{ae}_{8,12} = -\tfrac{19}{140} L^2 S^{ae}_{1,1},$$

$$K^{ae}_{9,2} = \tfrac{19}{70} L S^{ae}_{2,1}, \quad K^{ae}_{9,3} = \tfrac{19}{70} L S^{ae}_{3,2}, \quad K^{ae}_{9,4} = \tfrac{3}{20} L S^{ae}_{2,3}, \quad K^{ae}_{9,5} = -\tfrac{3}{70} L^2 S^{ae}_{2,2},$$

$$K^{ae}_{9,6} = \tfrac{3}{70} L^2 S^{ae}_{2,1},$$

$$K^{ae}_{9,8} = \tfrac{13}{35} L S^{ae}_{2,1}, \quad K^{ae}_{9,9} = \tfrac{13}{35} L S^{ae}_{2,2}, \quad K^{ae}_{9,10} = \tfrac{7}{20} L S^{ae}_{2,3}, \quad K^{ae}_{9,11} = \tfrac{19}{140} L^2 S^{ae}_{2,2},$$

$$K^{ae}_{9,12} = -\tfrac{19}{140} L^2 S^{ae}_{2,1},$$

$$K^{ae}_{10,2} = \tfrac{3}{20} LS^{ae}_{3,1}, \quad K^{ae}_{10,3} = \tfrac{3}{20} LS^{ae}_{3,2}, \quad K^{ae}_{10,4} = \tfrac{1}{6} LS^{ae}_{3,3}, \quad K^{ae}_{10,5} = -\tfrac{1}{30} L^2 S^{ae}_{3,2},$$

$$K^{ae}_{10,6} = \tfrac{1}{30} L^2 S^{ae}_{3,1},$$

$$K^{ae}_{10,8} = \tfrac{7}{20} LS^{ae}_{3,1}, \quad K^{ae}_{10,9} = \tfrac{7}{20} LS^{ae}_{3,2}, \quad K^{ae}_{10,10} = \tfrac{1}{3} LS^{ae}_{3,3}, \quad K^{ae}_{10,11} = \tfrac{1}{20} L^2 S^{ae}_{3,2},$$

$$K^{ae}_{10,12} = -\tfrac{1}{20} L^2 S^{ae}_{3,1},$$

$$K^{ae}_{11,2} = \tfrac{13}{210} L^2 S^{ae}_{2,1}, \quad K^{ae}_{11,3} = \tfrac{13}{210} L^2 S^{ae}_{2,2}, \quad K^{ae}_{11,4} = \tfrac{1}{30} L^2 S^{ae}_{2,3},$$

$$K^{ae}_{11,5} = -\tfrac{1}{140} L^2 S^{ae}_{2,2}, \quad K^{ae}_{11,6} = \tfrac{1}{140} L^2 S^{ae}_{2,1},$$

$$K^{ae}_{11,8} = \tfrac{19}{140} L^2 S^{ae}_{2,1}, \quad K^{ae}_{11,9} = \tfrac{19}{140} L^2 S^{ae}_{2,2}, \quad K^{ae}_{11,10} = \tfrac{1}{20} L^2 S^{ae}_{2,3},$$

$$K^{ae}_{11,11} = \tfrac{1}{105} L^2 S^{ae}_{2,2}, \quad K^{ae}_{11,12} = -\tfrac{1}{105} L^2 S^{ae}_{2,1},$$

$$K^{ae}_{12,2} = -\tfrac{13}{210} L^2 S^{ae}_{1,1}, \quad K^{ae}_{12,3} = -\tfrac{13}{210} L^2 S^{ae}_{1,2}, \quad K^{ae}_{12,4} = -\tfrac{1}{30} L^2 S^{ae}_{1,3},$$

$$K^{ae}_{12,5} = \tfrac{1}{140} L^2 S^{ae}_{1,2}, \quad K^{ae}_{12,6} = -\tfrac{1}{140} L^2 S^{ae}_{1,1},$$

$$K^{ae}_{12,8} = -\tfrac{19}{140} L^2 S^{ae}_{1,1}, \quad K^{ae}_{12,9} = -\tfrac{19}{140} L^2 S^{ae}_{1,2}, \quad K^{ae}_{12,10} = -\tfrac{1}{20} L^2 S^{ae}_{1,3},$$

$$K^{ae}_{12,11} = -\tfrac{1}{105} L^2 S^{ae}_{1,2}, \quad K^{ae}_{12,12} = \tfrac{1}{105} L^2 S^{ae}_{1,1}. \tag{A3}$$

in which $S^{ae}_{i,j}$ is the ij element of the matrix S^{ae}, and L the length of the element.

The aeroelastic damping coefficients in the 12×12 aeroelastic damping matrix, $\mathbf{C}^{ae}$, for the deck element can be derived according to equation (10). The resulting coefficients are the same as those in equation (A3) only if $K^{ae}_{i,j}$ and $S^{ae}_{i,j}$ are replaced by $C^{ae}_{i,j}$ and $D^{ae}_{i,j}$ respectively.

APPENDIX B. AERODYNAMIC ELEMENT FORCE MATRICES

According to equations (16) and (17), the force coefficients in the 12×2 matrix, $\mathbf{E}^b_d$, related to the buffeting forces at the nodal points of the deck element, can be derived as

$$E^b_d(1,1) = 0, \quad E^b_d(2,1) = C_{1,d} C_{D,d} L/U, \quad E^b_d(3,1) = C_{1,d} C_{L,d} L/U,$$

$$E^b_d(4,1) = C_{2,d} C_{M,d} L/U,$$

$$E^b_d(5,1) = -\tfrac{1}{6} C_{1,d} C_{L,d} L^2/U, \quad E^b_d(6,1) = \tfrac{1}{6} C_{1,d} C_{D,d} L^2/U, \quad E^b_d(7,1) = 0,$$

$$E^b_d(8,1) = C_{1,d} C_{D,d} L/U,$$

$$E^b_d(9,1) = C_{1,d} C_{L,d} L/U, \quad E^b_d(10,1) = C_{2,d} C_{M,d} L/U, \quad E^b_d(11,1) = \tfrac{1}{6} C_{1,d} C_{L,d} L^2/U,$$

$$E_d^b(12,1) = -\tfrac{1}{6}C_{1,d}C_{D,d}L^2/U,$$

$$E_d^b(1,2) = 0, \quad E_d^b(2,2) = \tfrac{1}{2}C_{1,d}C'_{D,d}L/U, \quad E_d^b(3,2) = \tfrac{1}{2}C_{1,d}(C'_{L,d} + C_{D,d})L/U,$$

$$E_d^b(4,2) = \tfrac{1}{2}C_{2,d}C'_{M,d}L/U,$$

$$E_d^b(5,2) = -\tfrac{1}{12}C_{1,d}(C'_{L,d} + C_{D,d})L^2/U, \quad E_d^b(6,2) = \tfrac{1}{12}C_{1,d}C'_{D,d}L^2/U,$$

$$E_d^b(7,2) = 0, \quad E_d^b(8,2) = \tfrac{1}{2}C_{1,d}C'_{D,d}L/U, \quad E_d^b(9,2) = \tfrac{1}{2}C_{1,d}(C'_{L,d} + C_{D,d})L/U,$$

$$E_d^b(10,2) = \tfrac{1}{2}C_{2,d}C'_{M,d}L/U, \quad E_d^b(11,2) = \tfrac{1}{12}C_{1,d}(C'_{L,d} + C_{D,d})L^2/U,$$

$$E_d^b(12,2) = -\tfrac{1}{12}C_{1,d}C'_{D,d}L^2/U. \tag{B1}$$

According to equations (20) and (21), the force coefficients in the 12×2 matrix, $\mathbf{E}_t^b$, related to the buffeting forces at the nodal points of the tower element can be expressed as

$$E_t^b(1,1) = 0, \quad E_t^b(2,1) = C_{1,t}C_{D,t}L/U, \quad E_t^b(3,1) = C_{1,t}C_{L,t}L/U,$$

$$E_t^b(4,1) = C_{2,t}C_{M,t}L/U,$$

$$E_t^b(5,1) = -\tfrac{1}{6}C_{1,t}C_{Lt}L^2/U, \quad E_t^b(6,1) = \tfrac{1}{6}C_{1,t}C_{D,t}L^2/U, \quad E_t^b(7,1) = 0,$$

$$E_t^b(8,1) = C_{1,t}C_{D,t}L/U,$$

$$E_t^b(9,1) = C_{1,t}C_{L,t}L/U, \quad E_t^b(10,1) = C_{2,t}C_{M,t}L/U, \quad E_t^b(11,1) = \tfrac{1}{6}C_{1,t}C_{L,t}L^2/U,$$

$$E_t^b(12,1) = -\tfrac{1}{6}C_{1,t}C_{D,t}L^2/U,$$

$$E_t^b(1,2) = 0, \quad E_t^b(2,2) = \tfrac{1}{2}C_{1,t}C'_{D,t}L/U, \quad E_t^b(3,2) = \tfrac{1}{2}C_{1,t}C'_{L,t}L/U,$$

$$E_t^b(4,2) = \tfrac{1}{2}C_{2,t}C'_{M,t}L/U,$$

$$E_t^b(5,2) = -\tfrac{1}{12}C_{1,t}C'_{L,t}L^2/U, \quad E_t^b(6,2) = \tfrac{1}{12}C_{1,t}C'_{D,t}L^2/U,$$

$$E_t^b(7,2) = 0, \quad E_t^b(8,2) = \tfrac{1}{2}C_{1,t}C'_{D,t}L/U, \quad E_t^b(9,2) = \tfrac{1}{2}C_{1,t}C'_{L,t}L/U$$

$$E_t^b(10,2) = \tfrac{1}{2}C_{2,t}C'_{M,t}L/U, \quad E_t^b(11,2) = \tfrac{1}{12}C_{1,t}C'_{L,t}L^2/U,$$

$$E_t^b(12,2) = -\tfrac{1}{12}C_{1,t}C'_{D,t}L^2/U. \tag{B2}$$

The interpolation function matrix $\mathbf{B}_c$ used for a cable element is as follows:

$$\mathbf{B}_c = \begin{bmatrix} 0 & 1 - x/L & 0 & 0 & x/L & 0 \\ 0 & 0 & 1 - x/L & 0 & 0 & x/L \end{bmatrix}. \tag{B3}$$

According to equations (24) and (25), the force coefficients in the 6×1 matrix, $\mathbf{E}_c^b$, related to the buffeting forces at the nodal points of the cable element can be obtained as

$$E_c^b(1,1) = E_c^b(4,1) = 0, \quad E_c^b(2,1) = E_c^b(5,1) = C_{1,c} C_{D,c} L/U,$$
$$E_c^b(3,1) = E_c^b(6,1) = C_{1,c} C_{L,c} L/U. \tag{B4}$$